ELSEVIER

Marine Geology 232 (2006) 35–47

MARINE GEOLOGY
INTERNATIONAL JOURNAL OF MARINE GEOLOGY, GEOCHEMISTRY AND GEOPHYSICS

www.elsevier.com/locate/margeo

Tsunamigenic sources in an active European half-graben (Gulf of Corinth, Central Greece)

Aristofanis Stefatos *, Marinos Charalambakis, George Papatheodorou [1], George Ferentinos [2]

Laboratory of Marine Geology and Physical Oceanography, Department of Geology, University of Patras, 26500 Rio Patras, Greece

Received 11 October 2005; received in revised form 9 June 2006; accepted 19 June 2006

Abstract

The Gulf of Corinth is an active half-graben dissecting the mainland of Greece along an east west axis. The Gulf is well known for its intense seismic activity and its rapid extension rates. However, published historical catalogues reveal that the Gulf of Corinth is also the site of frequent and relatively destructive tsunami occurrences.

This paper presents a comparative study of the potential of probable tsunami sources in the Gulf of Corinth, by referring to published offshore geology data. Coseismic seafloor displacement along offshore faults and submarine mass failures are the active tsunamigenic sources. The paper applies easy to use empirical and semi-empirical equations that estimate the generated tsunami wave height, just over the source area. Building upon the most probable worst-case scenarios for both coseismic fault-displacement and submarine mass failure generated tsunamis, the tsunami potential of its case is explored.

A maximum probable 6.7 (M_w) offshore earthquake would produce a rupture on the seafloor surface with a maximum displacement of 0.66 to 1.08 m in height in the Gulf of Corinth. The tsunami which would be generated by the seafloor displacement would have a wave height of the same magnitude as the seafloor displacement. Furthermore, existing evidence of submarine mass failures that took place over the last 3000 years in the eastern part of the Corinth Gulf had and would have the potential of generating tsunamis with a maximum wave height of 1.04 and 4.04 m and maximum wave length of 4.52 and 6.25 km.

Keywords: tsunami; offshore faulting; offshore slide; Corinth, Greece

1. Introduction

The December 2004 Indian Ocean tsunami has brought the need to assess tsunami hazards in various parts of the world, to the attention of the international community. Within the European Union, Greece not only has the highest seismicity record (McKenzie, 1978; Jackson and McKenzie, 1988; Ambraseys and Jackson, 1990) but is also situated in the eastern Mediterranean, an area that suffers the highest tsunami hazard within the EU zone. The analysis of historical records reveals a relatively

* Corresponding author. Tel.: +30 6976 405107; fax: +30 2610 991701.
E-mail addresses: a.stefatos@upatras.gr (A. Stefatos), cmarinos@upatras.gr (M. Charalambakis), George.Papatheodorou@upatras.gr (G. Papatheodorou), gferen@upatras.gr (G. Ferentinos).
[1] Tel./fax: 30 2610 996275.
[2] Tel.: +30 2610 997646; fax: +30 2610 991701.

0025-3227/$ - see front matter © 2006 Elsevier B.V. All rights reserved.
doi:10.1016/j.margeo.2006.06.004

increased high frequency of tsunami occurrence within the Gulf of Corinth, an enclosed marine basin in central Greece (Antonopoulos, 1980; Papadopoulos and Chalkis, 1984; Papazachos et al., 1986; Papadopoulos, 2003).

This paper evaluates the potential of the various tsunamigenic sources that are active within the Gulf of Corinth, a seismically active half-graben marine basin. Reviewing published and unpublished seafloor data, the paper applies tsunami generation models in order to estimate and compare the tsunami potential of each source. Using existing empirical and semi-empirical equations this paper builds a simple methodology for an initial, estimation of the potential tsunami hazard imposed by active offshore faults and submarine landslides.

2. Regional setting

The Gulf of Corinth is an active half-graben that dissects the Greek mainland along a WNW–ESE axis, over a distance of more than 130 km (Fig. 1). This elongated marine basin reaches a maximum depth of 900 m at its center and is characterized by steep north and south dipping slopes (8°–25°). Basin bounding faults control the extent of the shelf. The shelf is poorly developed, extending over distances of 20 to 2000 m and is under water depths of 100 to 200 m. Locally, in places such as the bays of Lechaio, Itea and Antikyra, the shelf extends as far as 8 to 16 km from the coast.

The basin boundaries to the north and south are fault controlled and host small and medium sized fan deltas. These footwall derived fan deltas develop along fault steps and constitute the principal clastic sediment input to the basin. The overall morphology of this narrow and deep marine basin remarkably resembles the setting of fjord-like basins found on higher latitudes.

The Gulf of Corinth is considered to be the submerged and most active sector of the Corinth rift that undergoes N–S extension, at a rate of 4–14 mm yr^{-1} (Billiris et al., 1991; Clarke et al., 1997; Briole et al., 2000). This high extension rate concentrated within the basin (Briole et al., 2000) is accommodated by the numerous offshore faults that are found in the area (Stefatos et al., 2002; McNeill et al., 2005) (Fig. 2). The rapid extension is accompanied by intense seismicity with a record of 30 earthquakes with a magnitude above 6 in the last 600 years (Ambraseys and Jackson, 1990, 1997; Papazachos and Papazachou, 1997; Papadopoulos, 2000) (Fig. 1b).

Active offshore and onshore faulting favours the development of submarine mass failures along the basins slopes. Especially in areas where river deltas develop, the

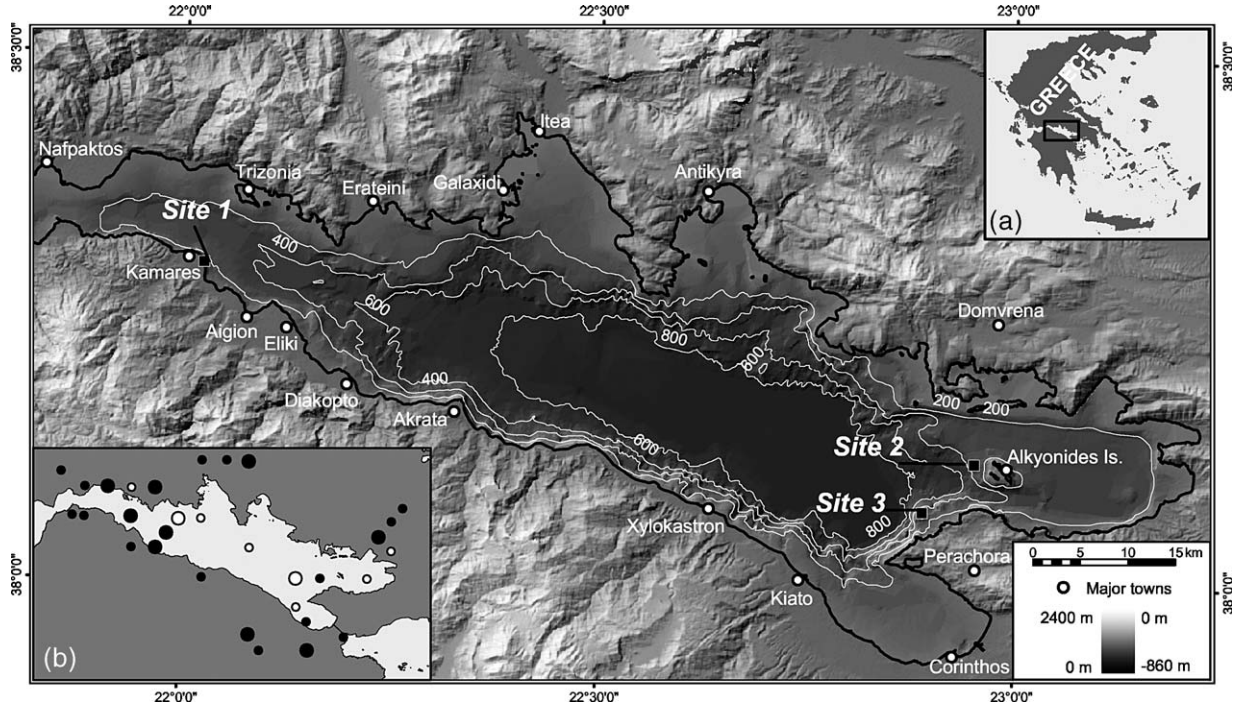

Fig. 1. Shaded relief map of the Gulf of Corinth and the surrounding land, showing locations of submarine slides discussed in the text. (a) An insert with Greece showing the geographical position of the Gulf of Corinth. (b) An insert with the epicenters of the 30 largest earthquakes over the last 600 years. Large symbols are events with $M_s > 6.5R$, smaller symbols are those with $6.0 < M_s < 6.5R$. Black circles represent events prior to 1900, white ones post-1900 events.

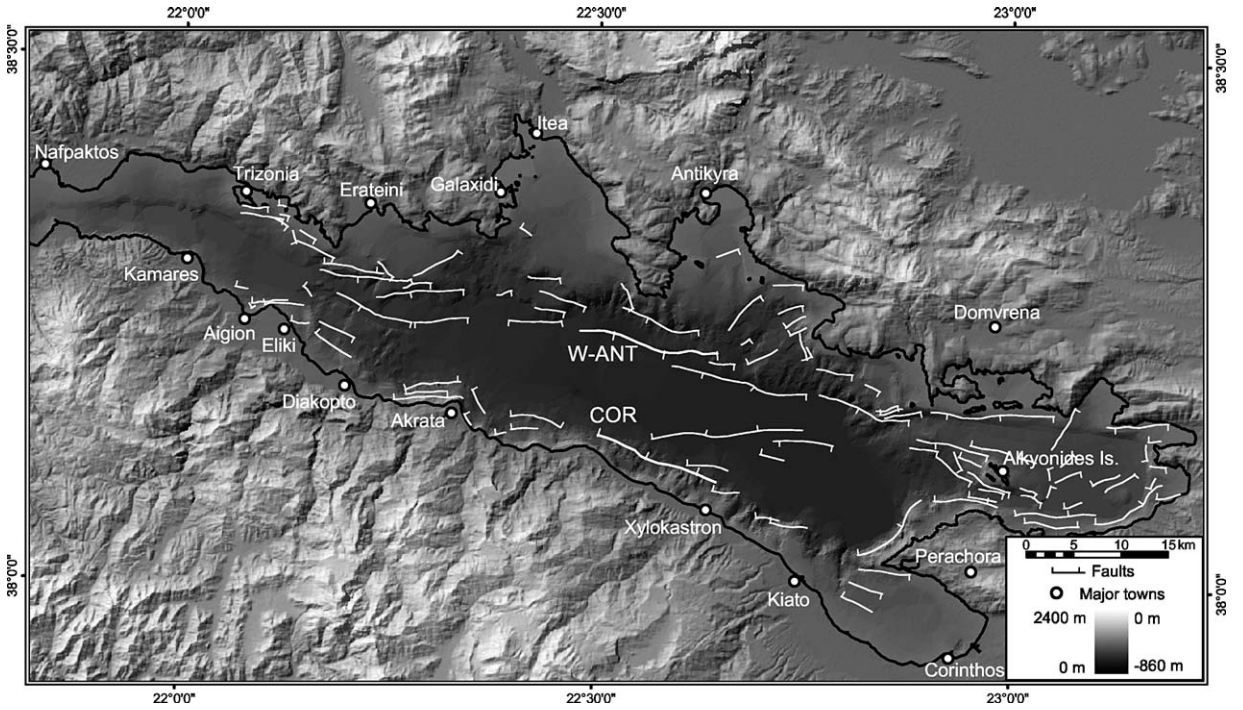

Fig. 2. New revised map of the offshore faults within the Gulf of Corinth (faults after Stefatos et al., 2002; Stefatos, 2005). Abbreviations: W-ANT, west-Antikyra fault; COR, Corinth Fault.

high sedimentation rates combined with intense earthquake shaking produce favourable conditions for the development of submarine mass failures. Such events have been thoroughly described by previous authors (Perissoratis et al., 1984; Ferentinos et al., 1988; Papatheodorou and Ferentinos, 1997; Hasiotis et al., 2002).

3. Tsunamis in the Gulf of Corinth

Over the years, a great number of tsunami catalogues for Greece, including the Gulf of Corinth, have been published by several authors (Heck, 1947; Galanopoulos, 1960; Ambraseys, 1962; Antonopoulos, 1980; Papadopoulos and Chalkis, 1984; Papazachos et al., 1986; Soloviev, 1990; Papadopoulos, 1993; Papazachos and Papazachou, 1997; Papadopoulos, 2000; Soloviev et al., 2000; Papadopoulos, 2003). The most recent catalogue reports a total of 17 probable and definite tsunami events, which have occurred within the Gulf of Corinth (Papadopoulos, 2003). With the exception of the first event of 373 BC, the remaining 16 out of 17 tsunami events are reported to have occurred since 1402. The frequency–intensity relationship indicates a 16, 40 and 103 year return period for at least one tsunami occurrence of intensity $TI \geq 2$, $TI \geq 3$ and $TI \geq 4$ respectively (Papadopoulos, 2003). Although the record regarding the actual wave height is incomplete the reported waves range in height between 0.5 and 10 m. Unfortunately there is no record of inundation distances, with the exception of the 1402 tsunami that struck the Central part of the Gulf and the well described 1963 tsunami in Kamares. The reported inundation distances for these two tsunamis are 1200 and 400 m respectively. It is worth noting that the reported structural damage and casualties were rather low.

The majority of the tsunamis are related to shallow earthquakes. However, it is not clear whether these waves were caused by the coseismic fault displacement on the seafloor or, by seismically triggered submarine and coastal sediment slides.

Four tsunami events in 1794, 1861, 1965 and 1984 are reported to have been generated by earthquake-triggered coastal landslides, one tsunami in 1888 is considered to have been caused by a seismically triggered submarine slide and two tsunamis in 1963 and 1996 are reported to have been triggered by aseismic coastal slides (Papadopoulos, 2003). The above-mentioned tsunami events demonstrate the necessity to further investigate the potential hazard imposed by such submarine landslides.

4. Seismic dislocation generated tsunamis

Coseismic seafloor displacement due to a shallow offshore earthquake can trigger a perturbation of the sea

surface. Considering that such deformation is much more rapid than the characteristic time required for wave propagation, and that the length scale of the seafloor deformation is much larger than the water depth, the approximation that initial sea-surface deformation is equal to the coseismic vertical displacement of the seafloor can be accepted (Geist and Dmowska, 1999; Hébert et al., 2005).

Accepting this approximation, the matters in question are what is the highest probable earthquake magnitude due to the activation of an offshore fault and what is the maximum coseismic fault displacement on the surface of the seafloor produced by such an earthquake. The vertical component of this seafloor displacement will constrain the magnitude of the tsunami generated.

4.1. Empirical average relationship approach

Marine seismic reflection surveys in the Gulf of Corinth have imaged numerous offshore faults with fault trace lengths up to 15 km long (Stefatos et al., 2002; Stefatos, 2005) (Fig. 2). Considering that, it is quite probable that a future large earthquake may rupture the entire length of any of these faults; empirical relationship equations are used to estimate the corresponding earthquake magnitude of such a fault rupture. Calculating surface displacement from rupture length is avoided since regressions between displacement and rupture length are less well correlated and have larger standard deviation than regressions between magnitude and length or displacement (Wells and Coppersmith, 1994).

Based on a worldwide record of historical earthquakes, Wells and Coppersmith (1994) proposed regression equation correlating trace length (L) and seismic moment magnitude (M_w):

$$M_w = 5.08 + 1.16\log(L) \quad (1)$$

Similar regression equations have been proposed by Pavlides and Caputo (2004) based on dataset of earthquakes from the broader Aegean region and by Ambraseys and Jackson (1998) based on a dataset from the eastern Mediterranean–Middle East Region (Eqs. (2) and (3) respectively):

$$M_s = 0.90\log(L) + 5.48 \quad (2)$$

$$M_s = 1.14\log(L) + 5.27 \quad (3)$$

Offshore fault data suggest that the Corinth offshore fault along the south margin and the west and east Antikyra faults along the north margin have a similar length of about 15 km (Fig. 2). This makes them the longest single fault traces within the Gulf of Corinth (nomenclature after Stefatos et al., 2002; faults modified after Stefatos, 2005; Charalambakis et al., 2005). Solving Eqs. (1), (2) and (3) for a maximum ruptured fault trace of 15 km, a maximum magnitude of *6.44*, *6.53* and *6.47* is respectively estimated.

It should be noted, that the estimated magnitude is slightly less than the maximum-recorded earthquake magnitude in the Gulf of Corinth. The maximum-recorded offshore earthquake shock in the Gulf of Corinth was the first in the series of three events that struck the eastern Gulf of Corinth in 1981. On February 24th 1981, a 6.7 (M_s), was recorded west of Alkyonides islands, northwest of Perachora Peninsula, at a focal depth of about 10 km (Jackson et al., 1982).

Considering our interest in estimating the worst-case scenario, the 6.7 magnitude earthquake is used as the maximum probable event in our analysis. To estimate the surface displacement produced by an earthquake of this magnitude the available regression equations correlating magnitude to surface displacement, are referred to.

Maximum surface displacement (MD) is related to earthquake magnitude through the regression equation (Wells and Coppersmith, 1994):

$$\log(\mathrm{MD}) = -5.46 + 0.82M_w \quad (4)$$

A similar equation, based on field observations from the broader Aegean region, correlates local magnitude (M_s) to maximum surface displacement (MD) (Pavlides and Caputo, 2004):

$$\log(\mathrm{MD}) = -7.82 + 1.14M_s \quad (5)$$

Solving Eqs. (4) and (5) for a magnitude value of 6.7 results in a 1.08 and 0.66 m maximum surface displacement along the fault trace. It should be noted that average surface displacement along the fault is considered to be approximately equal to one-half the maximum surface displacement (Wells and Coppersmith, 1994) and therefore using the maximum value of 1 m is thought to be a valid upper limit, suitable for exploring the worst-case scenario. The above predicted values of maximum surface displacement coincide well with those observed along faults surrounding the Corinth Gulf, which have been activated in the past (Jackson et al., 1982; Pirazzoli et al., 1994; Chatzipetros et al., 2005).

4.2. Fault specific approach

In a more conventional approach, the worst-case scenario should derive from a detailed fault specific

analysis of surface deformation produced during the occurrence of the maximum probable earthquake. In such a case the initial tsunami condition is directly obtained by applying the Okada's (1985) method for the calculation of the expected coseismic vertical deformation (Koshimura and Mofjeld, 2001; Borrero et al., 2004). In the present study it is assumed that the 6.7 (M_w) earthquake would occur along one of the two longest offshore fault segments; the 15.1 km long west-Antikyra fault or the 14.8 km long Corinth Fault (Fig. 2).

Assuming a 6.7 (M_w) earthquake on the Corinth or the west-Antikyra offshore faults, the analytical formulas established by Okada (1985) are used for the computation of the coseismic deformation caused, due to elastic dislocation of an inclined and tensile fault in half space. The fault parameters used for estimating the seismic deformation by the fault movement are shown in Table 1. The fault slip shown for the supposed 6.7 (M_w) earthquake is determined by the application of the empirical relationship:

$$\log(\mathrm{RLD}) = -1.88 + 0.5M_w \quad (6)$$

between magnitude and subsurface displacement proposed by Wells and Coppersmith (1994). In both cases the computed maximum vertical seismic displacement on the seafloor surface at any point along the fault would not exceed 0.7 m, which is less than the previously estimated 1.0 m.

4.3. Direct empirical approach (earthquake magnitude versus tsunami height)

Chick et al. (2001) working in Hauraki back-arc rift, in New Zealand, employed the empirical method of Abe (1995), to estimate the potential maximum tsunami height produced by the activation of the 16 km long, Kerepechi offshore fault.

Table 1
Dimensions of the Corinth and west-Antikyra offshore faults and source parameters of a 6.7 (M_w) earthquake scenario

Fault parameters	Corinth Fault	West-Antikyra fault
Length (km)	14.8	15.1
Width (km)	18.7	13.2
Depth (km)	12	12
Top edge depth (km)	0	0
Fault slip (m)	0.64	0.66
Strike	295°	102°
Dip angle	40°	65°
Rake	0°	197°

Fault parameters after Stefatos (2005) and Charalambakis et al. (2005). Fault slip after Wells and Coppersmith (1994).

The relevant equation for the predicted maximum tsunami wave height (H_t) in the Gulf of Corinth is:

$$\log H_t = \begin{cases} 0.5M_w - 3.30 + C & R \le R_o \\ M_w - \log R - 5.5 + C & R > R_o \end{cases} \quad (7)$$

where R is the distance from the epicenter in km, and $C=0.2$ for tsunami generation in a back-arc setting.

Applicability testing for locally generated tsunamis shows that this equation tends to over-predict maximum tsunami heights close to the epicenter (Abe, 1995). The distance R_o from the epicenter is defined as the radius of a circular generation area, equivalent to the area that is expected to be deformed by the earthquake. The radius R_o is given by equation:

$$\log R_o = 0.5M_w - 2.25 \quad (8)$$

By solving Eqs. (7) and (8) for $M_w=6.7$ we get a maximum tsunami height of 1.78 m within a 12.6 km radius from the epicenter. The predicted tsunami height is reduced to 0.82 m over a distance of 20 km from the epicenter.

Chick et al. (2001), also compared the results of the predictive empirical method by Abe (1995), with a two-dimensional depth-averaged finite-element model by Kawahara et al. (1978). Comparing their results the authors conclude that the Abe method predicts maximum wave heights 2 to 4 times higher than the finite-element method. However, since the numerical model was intended for deep water tsunami generation and also since it does not consider amplification by rupture within soft sediments, the Abe method results were considered to be a reasonable upper-bound for assessing the tsunami hazard (Chick et al., 2001). For the exact same reasons and because of the simplicity of the method the predictive equations of Abe (1995) were chosen for application in the case studied in the Gulf of Corinth.

5. Submarine mass failure generated Tsunamis

5.1. Tsunami generation model

In order to estimate the tsunami wave amplitude that is generated over the top of a submarine landslide, the semi-empirical equations of Watts et al. (2003) were used. These equations predict tsunami amplitude on the basis of the energetic scaling proposed by Watts (1998, 2000). The equations derive as curve fits of numerical experiments that were carried out on a complete fluids dynamics simulation of wave generation in two

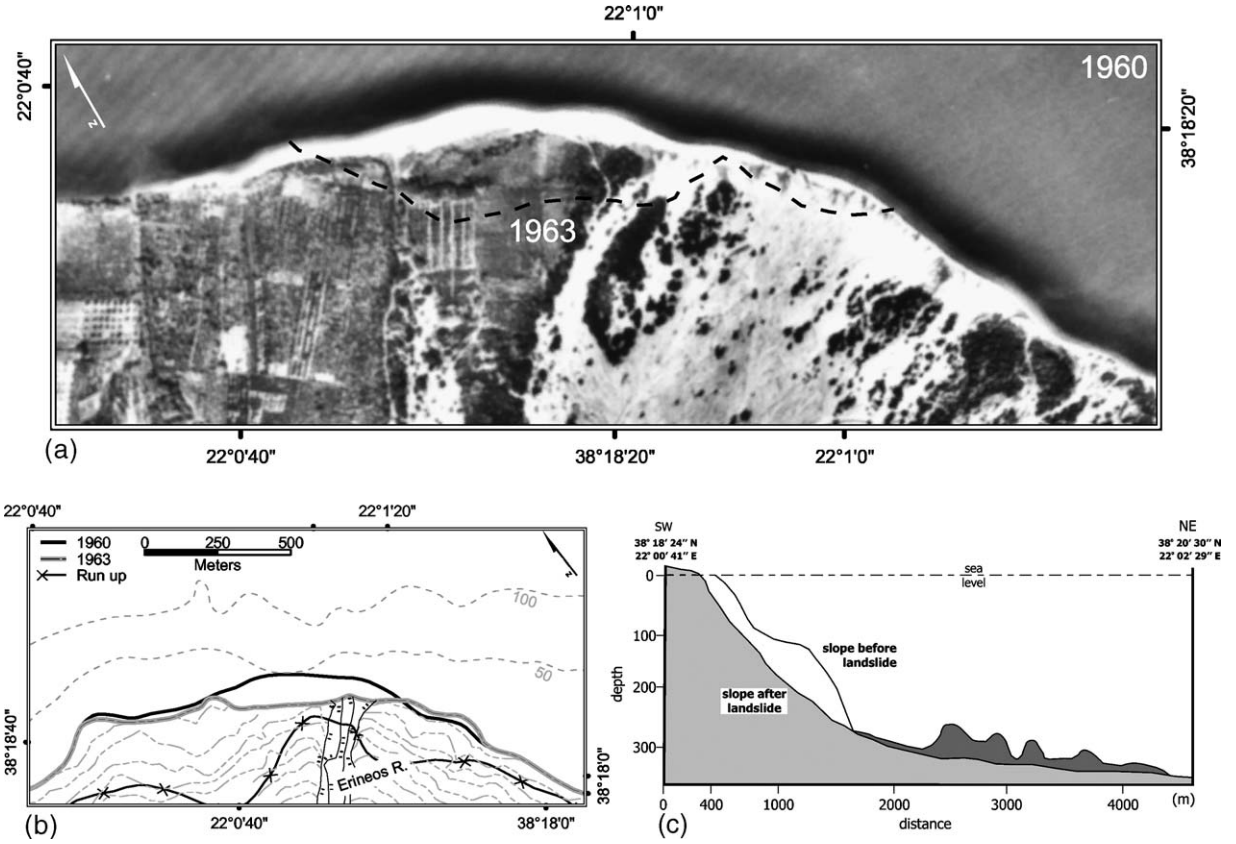

Fig. 3. (a) Aerial photograph of the Erineos river mouth, taken in 1963 before the occurrence of the coastal landslide. Dashed line indicates the shoreline position after the landslide. (b) Topographical chart of the area showing the runup distance and height of the tsunami (contours every 1 m). (c) Bathymetry profile offshore Erineos river mouth showing the alteration of the seafloor surface after the tsunami. All figures taken and modified after Galanopoulos et al., 1964.

dimensions using a boundary elements method (Grilli and Watts, 1999).

The predictive equations refer to a tsunami generation model that assumes a submarine mass failure of semi-elliptical shape sliding down a straight incline with angle θ from horizontal (Grilli and Watts, 1999; their Fig. 1). Since the model assumes negligible friction over the sliding surface, all predicted amplitudes should be considered maxima. The semi-ellipse has a maximum thickness T along half of the minor axis that is perpendicular to the major axis of total length b. The semi-ellipse is further described by its width (w) and its initial submergence (d) that corresponds to the initial water depth of the center of the sliding mass. The geometrical characteristics of the mass failure are required as input parameters for the equations and can be assessed using high-resolution seafloor acoustic imaging data.

Assuming a specific density $\gamma = 1.85$ for the submarine mass the relevant equations predict characteristic wavelength λ_o, over the characteristic time of motion (t_o), and 3-D tsunami wave height n_{3D}:

$$\lambda_o = t_o\sqrt{gd} \cong 3.87\sqrt{\frac{bd}{\sin\theta}} \tag{9}$$

$$n_{3D} \cong 0.2139T(1-0.7458\sin\theta + 0.1704\sin^2\theta)\left(\frac{b\sin\theta}{d}\right)^{1.25}\left(\frac{w}{w+\lambda}\right) \tag{10}$$

(Watts et al., 2003). Eqs. (9) and (10) describe the characteristic tsunami wave generated over the center of mass of the underwater slide (Watts et al., 2003). The equations are valid for $\theta < 30°$, $T/b > 0.2$ and $d/b > 0.06$.

Eq. (10) was originally derived for two-dimensional tsunami propagation and therefore tended to overestimate the actual three-dimensional tsunami amplitude. In order to correct the overestimated amplitude, the term $w/(w+\lambda)$ is included in Eq. (10) (Watts, 2004). Using the equations of motion given by Watts (1998, 2000),

Table 2
Tsunami source parameters for the Kamares 1963, submarine mass failure generated tsunami and the predicted tsunami wave parameters according to the tsunami generation model by Watts et al. (2003)

	Kamares slide	
Input parameters	γ	1.85
	b (m)	1495
	T (m)	49
	w (m)	630
	d (m)	87.5
	θ (m)	10°
Predicted values	α_o (m/s^2)	0.508
	u_t (m/s)	58.31
	s_o (m)	6692.7
	t_o (s)	114.77
	λ_o (m)	3.36
	η_o (m)	5.64

In descending order the parameters are, the specific density (γ), the initial landslide length (b), the maximum initial landslide thickness (T), the maximum landslide width (w), the mean initial landslide depth (d), and the mean initial slope angle (θ). The predicted outputs are the slide initial acceleration (α_o), the theoretical slide terminal velocity (u_t), the characteristic distance of the slide motion (s_o), the characteristic time of motion, (t_o), the wave length (λ_o), and the surface wave height above the middle of the initial slide (n_o).

the characteristic time of motion (t_o) as well as the initial acceleration of the slide (α_o), the characteristic speed (U_o) and distance (s_o) is calculated. Watts et al. (2000) and Watts (2004), who investigated the influence of slide deformation have shown that these equations of motion apply to deforming landslide center of mass motion and, that the impact on the characteristic tsunami amplitude is negligible.

The application of the predictive equations offers a simple and fast tool for the estimation of tsunami hazards and has been employed in quite a few studies around the world (Goldfinger et al., 2000; Tappin et al., 2001; Watts et al., 2003; McAdoo and Watts, 2004; McMurty et al., 2004).

5.2. The Kamares 1963 tsunami

On the night of February 7th, 1963, a coastal slide at the mouth of the Erineos river, generated a local tsunami that struck the adjacent coasts in the western Gulf of Corinth (site 1 in Fig. 1). Galanopoulos et al. (1964) who surveyed the area just after the incident, provide a rather detailed description of the coastal landslide and the produced tsunami wave. The survey of the area and the comparison of aerial photographs taken before and after the landslide, revealed a 630 m long and 100 m wide coastal zone that subsided beneath the sea surface (Galanopoulos et al., 1964) (Fig. 3). After the landslide the Hellenic Navy Hydrographic Service conducted a water depth survey in the area. According to their comparative seafloor profile before and after the landslide (Fig. 3), the main volume of the landslide mass was initially lying below the water and the submerged coastal zone corresponded to the upslope edge of the slide mass. Based on this data it is estimated that the landslide length along the slope was approximately 1495 m long, 630 m wide and 49 m thick. The initial water depth of the center of the failed sediment mass is estimated at 87.5 m and the mean slope angle at 10°.

Using the inferred geometry of the slide as input to the tsunami generation model a tsunami height of 5.64 m is estimated (Table 2). This wave height is remarkably close to the reported maximum wave that hit the area. Indeed, for the slide area adjacency a maximum runup height of 5 to 6 m was described (Fig. 3, Table 3).

5.3. Alkyonides–Perachora submarine landslides

In the eastern Gulf of Corinth, offshore the Perachora Peninsula and the Alkyonides islands, a series of submarine slides have been reported (Papatheodorou and Ferentinos, 1993). In the middle of the slope west of the Alkyonides islands (site 2, in Figs. 1, 4 and 5) a very well constrained evacuation zone of a submarine slide has been imaged (Papatheodorou and Ferentinos, 1993, their Figs. 7, 8 and 9). Side scan sonar and 3.5 kHz sub-bottom profiles, image a 900 m long by 1800 m wide evacuation zone lying over a slope dipping WSW at an average angle of 15°. Sharp, almost vertical sidewalls with a mean height of 40 m around the evacuation zone constrain its extent. Small hyperbolas on the slide plane and the absence of any indication of sediment cover indicate a relatively fresh slide surface. The corresponding water depth in the middle of the mass failure was 392 m. According to the geometrical characteristics of the mass failure the application of Eq. (10) predicts a tsunami with a wave height of 1.04 m and wave length of 4.52 km (Table 4).

Further to the south and west of the previous site, at the base of the slope of the Perachora Peninsula (site 3 in Figs. 1 and 4), three successive and partially stacked mass failure deposits lying on the basin floor have been mapped (Fig. 5). From top to bottom these deposits have volumes

Table 3
Predicted tsunami wave height and period and the reported wave height and period based on eyewitness accounts for the Kamares tsunami in 1963 (after Galanopoulos et al., 1964)

Input data	Predicted values	Actual observations
t_o (s)	114.77	≈120
η_o (m)	5.64	5–6

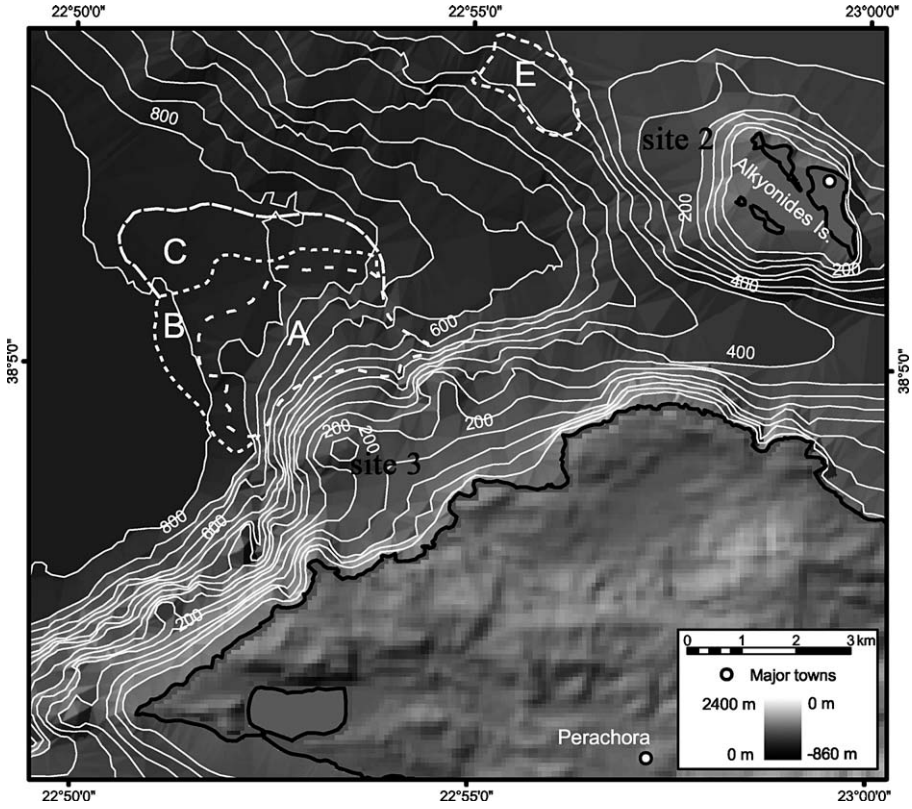

Fig. 4. Shaded relief map of the eastern Gulf of Corinth, showing the location of the Alkyonides submarine slide evacuation zone and the successive deposits of the Perachora submarine slides. Abbreviations: A, B and C Perachora slide deposits, E Alkyonides slide evacuation zone.

of 0.08, 0.12 and 0.15 km^3. In the seismic profiles a 2.5 to 5 m thick, veneer of well-layered sediments of hemipelagic and/or turbiditic origin covers these deposits. Considering that the present day and Holocene averaged sedimentation rates in the Gulf of Corinth is about 1.8 mm/year (Papatheodorou et al., 2003; Moretti et al., 2004), it is concluded that these submarine landslides took place about 1400 to 2800 years ago. These deposits have been related to slide evacuation zones on the adjacent slope, although the exact geometry has not been accurately defined.

Since the exact geometry of the initial mass is not known, existing average relationships that describe aspect ratios of landslides are referred to. Following the approach by Locat et al. (2004), as a reasonable approximation, the relationship proposed by Hungr (1988) relating the average flow depth (H_f) and slide volume (V) of a rock avalanche on land is accepted:

$$H_f = 0.05\ V^{0.33} \tag{11}$$

Indeed in this case the relationship returns an estimated slide thickness of 21.7 m, which is about one-half the thickness of the previously discussed submarine landslides.

Similarly in order to estimate an approximate reasonable length of the submarine slide, the approach of Watts (2004) who refers to the maximum thickness to initial length ratios of $T/b=0.5–5\%$ proposed for underwater slides is adopted (Prior and Coleman, 1979; Turner and Schuster, 1996). Since the source area size of underwater landslides in the Gulf of Corinth (Perissoratis et al., 1984; Papatheodorou and Ferentinos, 1997; Hasiotis et al., 2002) is close to the size of the landslides off the Mississippi delta (Prior and Coleman, 1979), the proposed ratio of 0.8% as the best estimate is adopted in this case. This ratio gives an initial slide length estimate of 2712 m. Then considering the assumption of the tsunami generation model, that the submarine slides have a semi-ellipsoid shape:

$$\left(V = \frac{\pi}{6} Tbw\right), \tag{12}$$

the width of the slide is estimated to be equal to 2596 m.

According to the above estimated geometrical characteristics of the submarine slide, if the slide was initiated

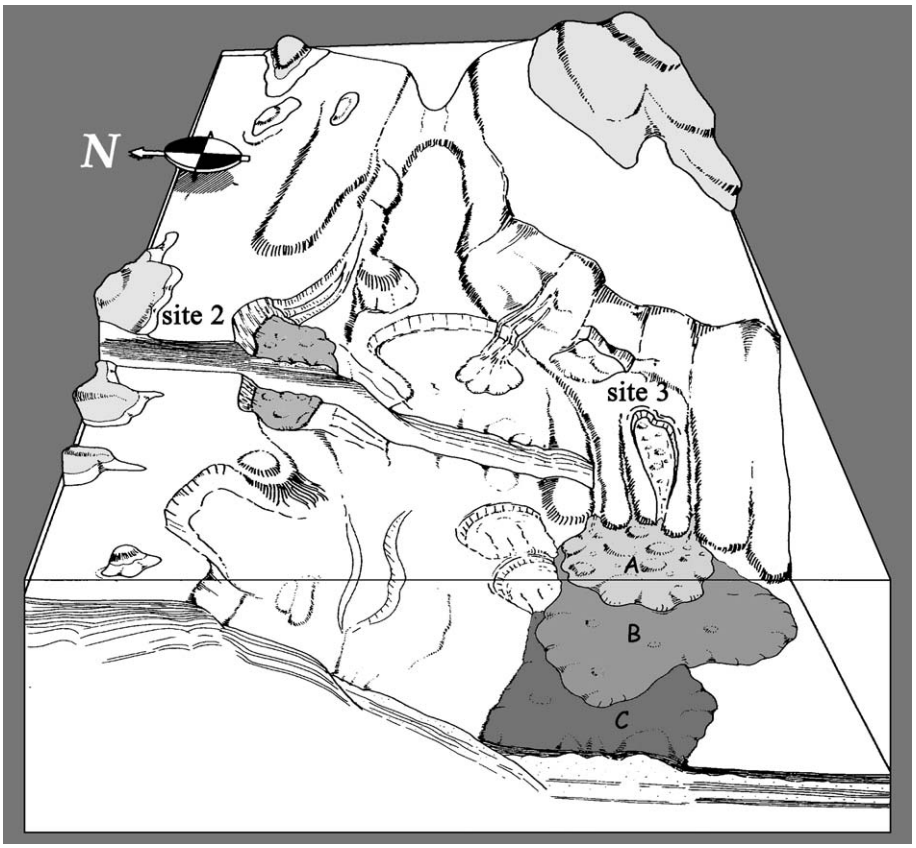

Fig. 5. Three dimensional representation of the eastern Gulf of Corinth, showing the geometry of the Alkyonides submarine slide evacuation zone (site 2) and the successive deposits of the Perachora submarine slides (site 3). Abbreviations: A, B and C Perachora slide deposits (modified after Papatheodorou and Ferentinos, 1993).

at approximately the shelf edge depth of 250 m and slid over the 15° slope, it would generate a tsunami wave 4.04 m high on the sea surface. In this case the estimated tsunami wavelength would be 6.27 km (Table 4).

6. Discussion

The above presented data have shown that: (i) the potential for a tsunami generation in the Corinth Gulf is high and (ii) the potential tsunamigenic sources are either coseismic seafloor displacement or coastal/submarine landslides.

The maximum expected coseismic seafloor displacement along the two longest active faults in the Corinth Gulf for earthquakes of M_w 6.7R, using three different approaches (Okada, 1985; Wells and Coppersmith, 1994; Abe, 1995; Pavlides and Caputo, 2004) ranges from 0.66 to 1.8 m (Table 5).

Considering that the direct empirical method of Abe (1995) does not take into account site-source specific data and because of its known tendency to overestimate the fault displacement, the estimated 1.8 m displacement is regarded as a rather improbable maximum value. Exclusion of the 1.8 m estimation narrows significantly the range of predicted values between 0.66 and 1.0 m. The analytical formulas of Okada (1985), and region-specific magnitude versus maximum displacement average relationship of Pavlides and Caputo (2004), result in very similar predictions at approximately 0.66 m. On the other hand, the magnitude versus maximum displacement curve fits of Wells and Coppersmith (1994) return an estimation of maximum surface displacement of 1.08 m. The expected coseismic seafloor displacement estimated using the Pavlides and Caputo (2004), Okada (1985) and Wells and Coppersmith (1994) regression equations coincides well with those observed on land faults of similar length bounding the Corinth Gulf which were activated in the past (Jackson et al., 1982; Pirazzoli et al., 1994; Chatzipetros et al., 2005). Therefore, the empirical equations by the above researchers are considered more appropriate to the direct method of Abe (1995).

Table 4
Eastern Gulf Of Corinth tsunami source parameters used as inputs to the tsunami generation model of Watts et al. (2003)

		Alkyonides slide	Alkyonides slide*	Perachora slide
Input parameters	γ	1.85	1.85	1.85
	b (m)	900	900	2712
	T (m)	40	40	21.7
	w (m)	1800	1800	2596
	d (m)	392	250	250
	θ (m)	15°	15°	15°
Predicted values	α_o (m/s^2)	0.757	0.757	0.757
	u_t (m/s)	55.24	55.24	95.88
	s_o (m)	4029.1	4029.1	12,141
	t_o (s)	72.94	72.94	126.6
	λ_o (km)	4.52	3.61	6.27
	η_o (m)	1.04	2.13	4.04

In descending order the parameters are, the specific density (γ), the initial landslide length (b), the maximum initial landslide thickness (T), the maximum landslide width (w), the mean initial landslide depth (d), and the mean initial slope angle (θ). The predicted outputs are the slide initial acceleration (α_o), the theoretical slide terminal velocity (u_t), the characteristic distance of the slide motion (s_o), the characteristic time of motion, (t_o), the wave length (λ_o), and the surface wave height above the middle of the initial slide (n_o).

Furthermore, since the fault specific approach with the application of the Okada (1985) model requires the input of fault parameters that are rather difficult to define and quite often unknown, the use of the Pavlides and Caputo (2004) and Wells and Coppersmith (1994) average empirical equations is considered a reasonable approximation valid for a rough investigation of worst-case scenarios in the Gulf of Corinth.

The tsunami expected wave height is considered to be approximately the same to the coseismic vertical displacement (Geist and Dmowska, 1999; Hébert et al., 2005), therefore it is expected to range between 0.66 and 1.8 m.

In order to determine the potential tsunami hazard from submarine slides in the Gulf of Corinth the semi-empirical equations of Watts et al. (2003) were employed in the analysis. The applicability of these equations was tested against the Kamares 1963 tsunami, and appears to provide a remarkably accurate estimate of both the generated tsunami maximum height and period.

Published seafloor data from the east Gulf of Corinth, indicate the existence of numerous submarine slides (Perissoratis et al., 1984; Papatheodorou and Ferentinos, 1993). The application of the tsunami prediction equations of Watts et al. (2003) in two of the most recent submarine slides, gives an estimation of the expected tsunami maximum wave heights of 1.04 and 4.04 m and maximum wavelengths of 4.52 and 6.27 km long (Table 6). These estimates are much higher than the estimation of a fault generated tsunami, even when compared to the overestimated tsunami heights predicted using Abe (1995) empirical method (Tables 5 and 6). It is therefore safe to conclude that, in the Gulf of Corinth, the potential tsunami hazard imposed by underwater slides is much higher than offshore fault generated tsunamis.

The tsunami source mechanism is difficult to be determined for historical events, the observed tsunamis, except for two, show a good correlation in time with the occurrence of local earthquakes. These cases are considered as earthquake triggered implying a fault dislocation mechanism source or an earthquake triggered landslide. According to the most recently revised catalogues of tsunami occurrences in the Gulf of Corinth, the tsunami heights reported range between 0.30 and 10 m (Papadopoulos, 2003). However, considering the results of this work, tsunamis with reported runup heights of 5 and 10 m should be treated with caution when determining the exact source mechanism. According to Stefatos et al. (2005) who applied a tsunami propagation model for tsunamis in the Gulf of Corinth, the amplification of the generated waves as they enter the shallow waters close to the shoreline does not exceed a factor of 1.2 anywhere along the coastline. It is therefore suggested, that the reported 5 to 10 m high tsunamis have been rather over-exaggerated by the people living on the time of the tsunami occurrence.

Up to present, the reported tsunamis seem that they have not caused any structural damage and the life losses were limited to one hand figures. This was apparently due to the fact that at those years the towns and villages in

Table 5
Resulting estimates of maximum vertical seafloor surface displacement during a 6.7 (M_w) earthquake

Wells and Coppersmith (1994)	Pavlides and Caputo (2004)	Okada (1985)	Abe (1995)
1.0 m	0.66 m	0.7 m	1.78 m

Such estimates are considered as being equal to initial sea-surface deformation and are used as initial conditions to tsunami propagation models. For the sake of comparison the estimations are presented against the estimation provided by the empirical equation of Abe (1995) for a direct maximum tsunami height prediction.

Table 6
Resulting estimates of tsunami heights for submarine mass failure generated tsunamis in the Gulf of Corinth

Kamares 1963	Alkyonides slide	Alkyonides slide*	Perachora slide
5.64 m	1.04 m	2.13 m	4.04 m

All predicted tsunami heights were calculated using the semi-empirical equations of Watts et al. (2003).

the lowlands around the Corinth Gulf were built sufficiently far away from the shoreline. However, considering the present day high tourism, which has resulted in the building of hotels and houses all along the Corinth Gulf shoreline, a similar size tsunami would cause many structural damage and loss of lives. For example, on a summer weekend an estimated 50,000 people gather along the beaches of the Corinth Gulf.

7. Concluding remarks

Although the relatively small sized, semi-enclosed, half-graben, marine basins, such as the Gulf of Corinth, do not host major fault zones similar to those found along the tectonic plate boundaries, these basins do suffer from a significant tsunami hazard. The tsunami hazard in this case is primarily related to local tsunamis generated by submarine slides.

The estimated wave height for the landslide-generated tsunamis significantly exceeds the expected height of the tsunamis generated by the coseismic seafloor dislocation along a fault. This conclusion is in accordance with the theoretical approach by Ruff (2003) and also the results of Hébert et al. (2005) for the Sea of Marmara and the California coastal zone (Watts, 2004).

The Wells and Coppersmith (1994) and the Pavlides and Caputo (2004) empirical equations provide reasonable rough estimations of fault generated tsunami height within the source area. Such estimations are considered valid for regional worst-case scenario studies. For a maximum probable offshore earthquake of 6.7 (M_w) in the Gulf of Corinth, the expected tsunami would have an initial wave height of about 1.0 m within the source area.

The easy to use semi-empirical equations by Watts et al. (2003) valid for submarine-failure generated tsunamis were tested against the well-described Kamares 1963 tsunami event. The model predictions are remarkably close to the actual observations, a fact that supports the validity of the model. Reviewing published data of submarine slides it is found that a potential mass failure at the shelf edge in the eastern Gulf of Corinth, similar in size to older failures, would generate an approximately 1.04–4.04 m high tsunami wave in the generation area.

The Corinth Gulf tsunamis are considered to have been local events some of which produced large waves that were locally destructive. The steep offshore morphology and the presence of under-consolidated alluvial sediments along the shelf favour the development of submarine landslides and therefore increase the potential of tsunamigenesis. The abundant record of tsunamis in the Gulf of Corinth supports this conclusion (Papadopoulos, 2000, 2003). The growth of population densities along the coasts over the last decades raises significant concern for a future tsunami event that could strike the Gulf of Corinth. Considering the numerous submarine mass failures reported around the Gulf of Corinth and the high frequency of tsunami occurrence it becomes more and more evident that detailed tsunami hazard assessment studies are needed in order to plan an effective civil protection policy for the area.

References

Abe, K., 1995. Estimate of tsunami run-up heights from earthquake magnitudes. In: Tsuchiya, Y., Shuto, N. (Eds.), Tsunami: Progress in Prediction, Disaster Prevention and Warning. Kluwer Academic Publishers, Dordrecht, pp. 21–35.

Ambraseys, N.N., 1962. Data for the investigation of the seismic sea-waves in the eastern Mediterranean. Bull. Seismol. Soc. Am. 52, 895–913.

Ambraseys, N.N., Jackson, J., 1990. Seismicity and associated strain of central Greece between 1980 and 1988. Geophys. J. Int. 101, 663–708.

Ambraseys, N.N., Jackson, J., 1997. Seismicity and strain in the Gulf of Corinth (Greece) since 1694. J. Earthqu. Eng. 1, 433–474.

Ambraseys, N.N., Jackson, J., 1998. Faulting associated with historical and recent earthquakes in the Eastern Mediterranean region. Geophys. J. Int. 133, 390–406.

Antonopoulos, J., 1980. Data from investigation on seismic sea-waves events in the eastern Mediterranean from birth of Christ to 1980 AD (6 parts). Annal. Geofis. 33, 141–248.

Billiris, H., Paradissis, D., Veis, G., England, P., Featherstone, W., Parsons, B., Cross, P., Rands, P., Rayson, M., Sellers, P., Ashkenazi, V., Davison, M., Jackson, J., Ambraseys, N., 1991. Geodetic determination of tectonic deformation in central Greece from 1900 to 1988. Nature 350, 124–129.

Borrero, J., Legg, M.R., Synolakis, C.E., 2004. Tsunami sources in the southern California bight. Geophys. Res. Lett. 31, L13211, doi:10.1029/2004GL020078.

Briole, P., Rigo, A., Lyon-Caen, H., Ruegg, J.C., Papazissi, C., Mitsakaki, C., Balodimou, A., Veis, G., Hatzfeld, D., Deschamps, A., 2000. Active deformation of the Corinth rift, Greece: results from repeated Global Positioning System surveys between 1990 and 1995. J. Geophys. Res. 105, 25,605–25,625.

Charalambakis, M., Stefatos, A., Hasiotis, T., Ferentinos, G., 2005. Morphology, structure and evolution of the Xylocastro basin bounding fault margin, central Gulf of Corinth. International Symposium on the Geodynamics of Eastern Mediterranean: Active Tectonics of the Aegean Region, 15–18 June 2005, Istanbul, Turkey.

Chatzipetros, A., Kokkalas, S., Pavlides, S., Koukouvelas, J., 2005. Paleoseismic data and their implication for active deformation in Greece. J. Geodyn. 40 (2–3), 170–188.

Chick, L.M., De Lange, W.P., Healy, T.R., 2001. Potential Tsunami hazard associated with the Kerepechi Fault, Firth of Thames, New Zealand. Nat. Hazards 24, 309–318.

Clarke, P.J., Davies, R.R., England, P.C., Parsons, B.E., Billiris, H., Paradissis, D., Veis, G., Denys, P.H., Cross, P.A., Ashkenazi, V., Bingley, R., 1997. Geodetic estimate of seismic hazard in the Gulf of Korinthos. Geophys. Res. Lett. 24, 1303–1306.

Ferentinos, G., Papatheodorou, G., Collins, M.B., 1988. Sediment transport processes on an active submarine fault escarpment: Gulf of Corinth, Greece. Mar. Geol. 83, 43–61.

Galanopoulos, A.G., 1960. Tsunamis observed on the coasts of Greece from antiquity to present time. Ann. Geofis. 13, 369–386.

Galanopoulos, A., Delimbasis, N.D., Comninakis, P.E., 1964. A tsunami generated by a slide without a seismic shock. Geological Chronicles of Greece, vol. 16, pp. 93–110 (in Greek).

Geist, E.L., Dmowska, R., 1999. Local tsunamis and distributed slip at the source. Pure Appl. Geophys. 154, 485–512.

Goldfinger, G., Kulm, D., McNeil, L., Watts, P., 2000. Super-scale failure of the Southern Oregon Cascadia Margin. Pure Appl. Geophys. 157, 1189–1222.

Grilli, S., Watts, P., 1999. Modelling of waves generated by a moving submerged body: applications to underwater landslides. Eng. Anal. Bound. Elem. 23, 645–656.

Hasiotis, T., Papatheodorou, G., Bouckovalas, G., Corbau, C., Ferentinos, G., 2002. Earthquake-induced coastal sediment instabilities in the western Gulf of Corinth, Greece. Mar. Geol. 186, 319–335.

Heck, N., 1947. List of seismic sea-waves. Bull. Seismol. Soc. Am. 37, 270.

Hébert, H., Schindelé, F., Altinok, Y., Alpar, B., Gazioglu, C., 2005. Tsunami hazard in the Marmara Sea (Turkey): a numerical approach to discuss active faulting and impact on the Istanbul coastal areas. Mar. Geol. 215, 23–43.

Hungr, O., 1988. Dynamics of rock avalanches and types of slope movements. Ph.D. thesis, University of Alberta, Edmonton, AB.

Jackson, J.A., McKenzie, D.P., 1988. The relationship between plate motions and seismic tensors and the rate of active deformation in the Mediterranean and Middle East. Geophys. J. 93, 45–73.

Jackson, J.A., Cagnepain, J., Houseman, G., King, J., Papadimitriou, P., Soufleris, G., Virieux, J., 1982. Seismicity, normal faulting and the geomorphological development of the Gulf of Corinth (Greece): the Corinth earthquakes of February and March 1981. Earth Planet. Sci. Lett. 57, 377–392.

Kawahara, M., Takeuchi, N., Yoshida, T., 1978. Two step explicit finite element method for tsunami wave propagation analysis. Int. J. Numer. Methods Eng. 12, 331–351.

Koshimura, S., Mofjeld, H., 2001. Inundation modeling of local tsunamis in Puget Sound, Washington, due to potential earthquakes. International Tsunami Symposium Proceedings, 8–9 August, Seattle, pp. 861–873.

Locat, J., Lee, H.J., Locat, P., Imran, J., 2004. Numerical analysis of the mobility of the Palos Verdes debris avalanche, California, and its implication for the generation of tsunamis. Mar. Geol. 203, 269–280.

McAdoo, B.G., Watts, P., 2004. Tsunami hazard from submarine landslides on the Oregon continental slope. Mar. Geol. 203, 235–245.

McKenzie, D., 1978. Active tectonics of the Alpine–Himalayan belt: the Aegean Sea and surrounding regions. Geophys. J. R. Astron. Soc. 55, 217–254.

McMurty, G.M., Watts, P., Fryer, G.J., Smith, J.R., Imamura, F., 2004. Giant landslides, mega-tsunamis, and paleo-sea level in the Hawaiian Islands. Mar. Geol. 203, 219–233.

McNeill, L.C., Cotterill, C.J., Henstock, T.J., Bull, J.M., Stefatos, A., Collier, R.E.L., Papatheoderou, G., Ferentinos, G., Hicks, S.E., 2005. Active faulting within the offshore western Gulf of Corinth, Greece: implications for models of continental rift deformation. Geology 33, 241–244.

Moretti, I., Lykousis, V., Sakellariou, D., Reynaud, J.-Y., Benziane, B., Prinzhoffer, A., 2004. Sedimentation and subsidence rate in the Gulf of Corinth: what we learn from the Marion Dufrense's long-piston coring. C.R. Geoscience 336, 291–299.

Okada, Y., 1985. Surface deformation due to shear and tensile faults in a half-space. Bull. Seismol. Soc. Am. 75, 1135–1154.

Papadopoulos, G.A., 1993. On some exceptional seismic (?) sea-waves in the Greek Archipelago. Science of Tsunami Hazard 11, 25–34.

Papadopoulos, G.A., 2000. A new tsunami catalogue of the Corinth Rift: 373 B.C.–A.D. 2000. In: Papadopoulos, G.A. (Ed.), Historical Earthquakes and Tsunamis in the Corinth Rift, Central Greece. Inst. Geodynamics, Natural Observatory, Athens, pp. 121–126.

Papadopoulos, G.A., 2003. Tsunami hazard in the eastern Mediterranean: strong earthquakes and tsunamis in the Corinth Gulf Central Greece. Nat. Hazards 29, 437–464.

Papadopoulos, G.A., Chalkis, B., 1984. Tsunamis observed in Greece and the surrounding area from antiquity up to the present times. Mar. Geol. 56, 309–317.

Papatheodorou, G., Ferentinos, G., 1993. Sedimentation processes and basin-filling depositional architecture in an active asymmetric graben: Strava graben, Gulf of Corinth, Greece. Basin Res. 5, 235–253.

Papatheodorou, G., Ferentinos, G., 1997. Submarine and coastal sediment failure triggered by the 1995, M_s=6.1 R Aegion earthquake, Gulf of Corinth, Greece. Mar. Geol. 137, 287–304.

Papatheodorou, G., Stefatos, A., Christodoulou, D., Ferentinos, G., 2003. Small scale present day turbidity currents in a tectonically active submarine graben, the Gulf of Corinth (Greece): their significance in dispersing mine tailings and their relevance to basin filling. In: Locat, J., Mienert, J. (Eds.), Submarine Mass Movements and their Consequences. Kluwer Academic Publishers, Dordrecht, pp. 459–468.

Papazachos, B., Papazachou, C., 1997. Earthquakes in Greece, Ekdoseis Ziti, Thessaloniki.

Papazachos, B., Koutitas, Ch., Hatzidimitriou, P., Karakostas, B., Papaioannou, C., 1986. Tsunami hazard in Greece and the surrounding area. Ann. Geophys. 4, 79–90.

Pavlides, S., Caputo, R., 2004. Magnitude versus fault's surface parameters: quantitative relationships from the Aegean Region. Tectonophysics 380, 159–188.

Perissoratis, C., Mitropoulos, D., Angelopoulos, J., 1984. The role of earthquakes in inducing sediments mass movements in the eastern Corinthiakos Gulf: an example from the February 24–March 4, 1981 activity. Mar. Geol. 55, 35–45.

Pirazzoli, P., Stiros, S., Arnold, M., Laborel, J., Laborel Derguen, F., Papageorgiou, S., 1994. Episodic uplift deduced from Holocene shorelines in the Perachora Peninsula, Corinth area, Greece. Tectonophysics 299, 201–209.

Prior, D., Coleman, J., 1979. Submarine landslides: geometry and nomenclature. Z. Geomorph. N.F. 23, 415–426.

Soloviev, S.L., 1990. Tsunamigenic zones in the Mediterranean sea. Nat. Hazards 3, 183–202.

Soloviev, S.L., Solovieva, O.N., Go, C.N., Kim, K.S, Shchetnikov, N.A., 2000. Tsunamis in the Mediterranean Sea — 2000 B.C.–2000 A.D. Kluwer Academic Publishers, Dordrecht. 237 pp.

Stefatos, A., 2005. Study of sedimentary processes and tectonic structure in the Gulf of Corinth with the use of marine geophysical methods. PhD Thesis, University of Patras, Patras, 221 pp.

Stefatos, A., Papatheodorou, G., Ferentinos, G., Collier, M., 2002. Seismic reflection imaging of active offshore faults in the Gulf of Corinth: their seismotectonic significance. Basin Res. 14, 487–502.

Stefatos, A., Charalambakis, M., Papatheodorou, G., Ghionis, G., Ferentinos, G., 2005. Potential tsunami hazard from submarine landslides in the Gulf of Corinth, Corinth. In: Papadopoulos, G.A., Satake, K. (Eds.), 22nd International Tsunami Symposium Proceedings, 27–29 June, Chania, pp. 233–240.

Tappin, D.R., Watts, P., McMurty, G.M., Lafoy, Y., Matsumoto, T., 2001. The Sissano, Papua New Guinea tsunami of July 1998 — offshore evidence on the source mechanism. Mar. Geol. 175, 1–23.

Turner, A.K., Schuster, R.L., 1996. Landslides: investigation and mitigation. Spec. Rep., vol. 247. Trans. Res. Board, National Academy Press, Whasington, DC.

Ruff, L.J., 2003. Some aspects of energy balance and tsunami generation by earthquakes and landslides. Pure Appl. Geophys. 160, 2155–2176.

Watts, P., 1998. Wavemaker curves for tsunamis generated by underwater landslides. J. Waterw. Port Coast. Ocean Eng. ASCE 124, 127–137.

Watts, P., 2000. Tsunamis features of solid block underwater landslides. J. Waterw. Port Coast. Ocean Eng. ASCE 126, 144–152.

Watts, P., 2004. Probabilistic predictions of landslide tsunamis off southern California. Mar. Geol. 203, 281–301.

Watts, P., Imamura, F., Grilli, S.T., 2000. Comparing model simulations of three benchmark tsunami generation cases. Sci. Tsunami Hazards 18, 107–124.

Watts, P., Grilli, S.T., Kirby, J.T., Fryer, G.J., Tappin, D.R., 2003. Landslide tsunami case studies using a Boussinesq model and a fully nonlinear tsunami generation model. Nat. Hazards Earth Syst. Sci. 3, 391–402.

Wells, D.L., Coppersmith, K.J., 1994. New empirical relationships among magnitude, rupture length, rupture width, rupture area and surface displacement. Bull. Seismol. Soc. Am. 84, 974–1002.